

# SPIN MATCHING FOR THE EIC'S ELECTRONS\*

M. G. Signorelli<sup>1†</sup>, G. H. Hoffstaetter<sup>1,2</sup>, J. Kewisch<sup>2</sup>, J. A. Crittenden<sup>1</sup>

<sup>1</sup> Cornell University, Ithaca, NY, USA

<sup>2</sup> Brookhaven National Laboratory, Upton, NY, USA

## Abstract

The Electron-Ion Collider (EIC) at Brookhaven National Laboratory will provide spin-polarized collisions of electron and protons or light ion beams. In order to maximize the electron polarization and require less frequent beam re-injections to restore the polarization level, the stochastic depolarizing effects of synchrotron radiation must be minimized via spin matching. In this study, Bmad was used to perform first order spin matching in the Electron Storage Ring (ESR) of the EIC. Spin matches were obtained for the rotator systems and for a vertical chicane, inserted as a vertical emittance creator. Monte Carlo spin tracking with radiation was then performed to analyze the effects of the spin matching on the polarization.

## INTRODUCTION

The Electron-Ion Collider (EIC) at Brookhaven National Laboratory will explore a new frontier in nuclear physics experiments by allowing for spin-polarized collisions of electrons and light ions. The electron beam will be stored in a new ring, the electron storage ring (ESR) of the EIC; this lattice must be designed to give maximum longitudinal polarization at the interaction points (IPs) for various electron beam energies between 5-18 GeV. The Thomas-BMT equation, shown in Eq. (1), defines the spin dynamics of a charged particle moving relativistically through laboratory-frame magnetic fields, where  $\vec{S}$  is a 3-vector of the spin expectation values in each direction [1–3].

$$\frac{d\vec{S}}{dt} = -\frac{q}{\gamma m} [(1 + a\gamma)\vec{B}_\perp + (1 + a)\vec{B}_\parallel] \times \vec{S} \quad (1)$$

The dynamics of this equation may be linearized in small phase space variables around the closed orbit, so that transfer through a lattice element is simply a multiplication of the original spin vector by some rotation matrix  $R(\theta; \theta_0, \vec{z}_0)$  where  $\theta_0$  and  $\theta$  are the initial and final azimuthal angles around the ring respectively and  $\vec{z}_0$  is the initial 6-dimensional phase space coordinate. Thus, if on the closed orbit  $\vec{z}_{c.o.}$ , the periodic spin direction can be defined in Eq. (2) [4, 5].

$$\hat{n}_0 = R(\theta_0 + 2\pi; \theta_0, \vec{z}_{c.o.})\hat{n}_0 \quad (2)$$

The primary task in designing any polarized storage ring is ordering lattice elements so that  $\hat{n}_0$  is rotated to point in

the desired direction at each position, while also accounting for spin resonances. However, when designing a lepton ring, the stochastic emission of synchrotron radiation has several significant effects on polarization that must be accounted for; firstly, derivable from the Dirac equation, the Sokolov-Ternov effect is an asymmetrical spin flip of electrons during photon emission, with higher probability of flipping antiparallel to the magnetic field [6]. This phenomenon can be taken advantage of to improve the polarization in a ring, as over time most of the spins will align antiparallel to the vertical field. The second and not as convenient effect is that of spin diffusion; when an electron emits a photon in a dipole, it experiences a sudden quantum reduction in energy. This instantaneously changes the equilibrium orbit of the particle, thus exciting synchrotron oscillations around this new orbit. Because the spin precession is coupled with orbit motion, there is a diffusion of the spin from the stable spin direction. Finally, when there is photon emission without a spin flip, there will be an instantaneous increase in alignment of the spin with  $\hat{n}_0$  - “kinetic polarization” [7].

Baier, Katkov, and Strakhovenko (BKS) derived expressions for the asymptotic polarization and build up time in a storage ring caused by the Sokolov-Ternov effect, and their work was then extended by Derbenev and Kondratenko (DK) to include spin diffusion and kinetic polarization [8–10]. Equation (3) gives the polarization time evolution from initial polarization  $P_0$  to asymptotic  $P_{dk}$ , and Eq. (4) gives the time constant in terms of the polarization buildup and depolarization rates [11].

$$P(t) = P_{dk} (1 - e^{-t/\tau_{dk}}) + P_0 e^{-t/\tau_{dk}} \quad (3)$$

$$\tau_{dk}^{-1} = \tau_{pol}^{-1} + \tau_{dep}^{-1} \quad (4)$$

While the analytical forms exist, it is difficult to actually calculate accurate results for  $P_{dk}$  and  $\tau_{dk}^{-1}$ . Thus,  $\tau_{dep}^{-1}$  is best obtained by Monte Carlo spin tracking without spin-flip effects [12]. Analytically calculating  $P_{bks}$  and  $\tau_{pol}^{-1} \approx \tau_{bks}^{-1}$ ,  $P_{dk}$  may then be sufficiently approximated with Eq. (5).

$$P_{dk} \approx P_{bks} \frac{\tau_{bks}^{-1}}{\tau_{bks}^{-1} + \tau_{dep}^{-1}} \quad (5)$$

Spin-orbit coupling, and dependence on energy, may be shown via a perturbative approach of the momentum deviation in the Thomas-BMT equation. To first order, the Thomas-BMT equation can be expressed as Eq. (6) in terms of the closed orbit spin precession  $\vec{\Omega}_{c.o.}$  and the phase space dependent perturbative precession  $\vec{\omega}$ , where  $s$  is the longitudinal position,  $\delta = \Delta p/p_0$ , and  $K_y$ ,  $K_1$ ,  $\tilde{K}_1$ , and  $K_s$  are the normalized dipole, quadrupole, skew quadrupole, and

\* This work was supported by the U.S. Department of Energy, Office of Science, Office of Workforce Development for Teachers and Scientists under the Science Undergraduate Laboratory Internships Program, and by Brookhaven Science Associates, LLC under Contract Nos. DE-SC0012704 and DE-SC0018370 with the U.S. Department of Energy.  
† mgs255@cornell.edu

solenoid strengths respectively. Substitution of the equations of motion and a bit of mathematical manipulation gives two equivalent expressions for  $\vec{\omega}$ , either of which may serve more useful than the other in certain circumstances [13].

$$\frac{d\vec{S}}{ds} = \left[ \vec{\Omega}_{c.o.}(s; s_0, \vec{z}_{c.o.}) + \vec{\omega}(s; s_0, \vec{z}) \right] \times \vec{S} \quad (6)$$

$$\omega_x = (1 + a\gamma_0)y'' + (1 + a)K_s x' \quad (7a)$$

$$\omega_s = (1 + a)(K_y' y - K_s \delta) - a(\gamma_0 - 1)K_y y' \quad (7b)$$

$$\omega_y = -(1 + a\gamma_0)x'' + a\left(\gamma_0 - \frac{1}{\gamma_0}\right)K_y \delta + (1 + a)K_s y' \quad (7c)$$

$$\omega_x = (1 + a\gamma_0)\left(K_1 y - \tilde{K}_1 x - \frac{1}{2}K_s' x\right) - a(\gamma_0 - 1)K_s x' \quad (8a)$$

$$\omega_s = (1 + a\gamma_0)(K_y' y - K_s \delta) - a(\gamma_0 - 1)(K_y y' + K_y' y - K_s \delta) \quad (8b)$$

$$\omega_y = (1 + a\gamma_0)\left(K_y^2 x + K_1 x + \tilde{K}_1 y - \frac{1}{2}K_s' y\right) - a(\gamma_0 - 1)K_s y' - \left(1 + \frac{a}{\gamma_0}\right)K_y \delta \quad (8c)$$

In order to remedy the depolarizing effects of spin diffusion, the dependence of  $\hat{n}$  with particle energy must be minimized; ideally,  $\vec{d} = \partial\hat{n}/\partial\delta = 0$  around the ring. However, whenever any sort of spin rotator exists in the lattice,  $\vec{d}$  will be excited and nonzero [14]. Thus, the goal is to ensure that this excitation of  $\vec{d}$  is local, so that  $\vec{d} = 0$  outside of any spin rotator system. In this work, the spin rotator system in a preliminary 1 IP 17.84 GeV ESR lattice was spin matched computationally using Bmad/Tao, and compared to the spin match obtained by an analytical derivation [15] assuming  $(1 + a) \approx 1$ . Then a localized vertical dispersion bump - a vertical chicane - was inserted into the lattice in a drift space to increase vertical emittance and fix the electron-ion beam size mismatch. This bump was vertically spin matched using Bmad/Tao, and the effects of the spin match were explored by Monte Carlo spin tracking with radiation.

For the ESR lattice investigated,  $\hat{n}_0$  is rotated from the vertical to the longitudinal using two solenoid modules on each side of the IP, designated by the blue cylinders in the top diagram of Figure 1. Each solenoid module consists of

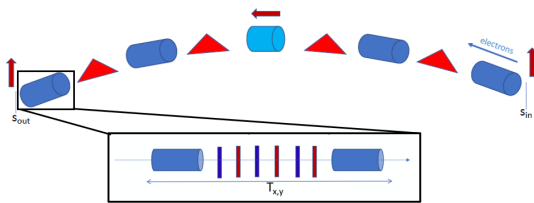


Figure 1: Schematic of the spin rotator system used in the preliminary 1 IP ESR lattice investigated in this work [16].

two equivalent solenoids separated by either 7 quadrupoles for the module closer to the IP, or 6 quadrupoles for the one closer to the arc. These are separated by bending modules, specified by the red diamonds in Figure 1. By varying the strengths of the solenoids,  $\hat{n}_0$  can be rotated to the longitudinal at the IP for various energies between 5-18 GeV.

## METHODS

Bmad/Tao utilizes the SLIM formalism, developed by Chao, for spin matching [17]. To first order, deviations of spin from the stable spin direction  $\hat{n}_0$  caused by spin-orbit motion can be expressed as  $\vec{S} \approx n_0 + \alpha\hat{l}_0 + \beta\hat{m}_0$ , where  $(\hat{l}_0, \hat{m}_0, \hat{n}_0)$  forms an orthonormal basis and  $\alpha$  and  $\beta$  are small. The propagation of  $\alpha$  and  $\beta$  are expressed by extending the 6x6 matrix formalism to an 8x8 matrix formalism as in Eq. (9), where the  $\mathbf{G}$  matrices define the spin-orbit coupling in the  $x$ ,  $y$ , and  $s$  directions and  $\mathbf{D}$  defines the closed orbit spin transport [12]. Varying optical elements so that  $\mathbf{G} = 0$  is thus performing first order spin matching.

$$\begin{pmatrix} \vec{z} \\ \alpha \\ \beta \end{pmatrix} = \begin{pmatrix} \mathbf{M}_{6 \times 6} & \mathbf{0}_{6 \times 2} \\ \mathbf{G}_{2 \times 6} & \mathbf{D}_{2 \times 2} \end{pmatrix} \begin{pmatrix} \vec{z}_0 \\ \alpha_0 \\ \beta_0 \end{pmatrix} \quad (9)$$

Radiation damping and fluctuations were included for all lattices, and the resulting ‘‘sawtooth’’ closed orbit fixed with the ‘‘taper’’ command in Bmad/Tao, which varies each magnet slightly to zero the orbit as much as possible. First, the rotator system was horizontally spin matched by varying the strengths of the quadrupoles between the solenoids in each module until  $\mathbf{G}_x = 0$  across the rotator. Then, after inserting the vertical chicane, all quadrupoles outside of the rotator were used to obtain a vertical spin match  $\mathbf{G}_y = 0$  across the ring from the center of the chicane. Finally, Bmad tracking of 1,000 particles for 10,000 turns with radiation was performed to analyze the polarization and vertical emittance.

## RESULTS

Table 1: The  $\mathbf{G}_x$  matrix across the ESR spin rotator with optics satisfying the analytical conditions [15] and optics computationally spin matched in Bmad/Tao.

Analytical	Computational
$\begin{pmatrix} 0.0000120 & 0.0005214 \\ 0.0018243 & 0.0075423 \end{pmatrix}$	$\begin{pmatrix} 0.0000000 & 0.0000000 \\ 0.0000000 & 0.0000000 \end{pmatrix}$

As shown in Table 1, the  $\mathbf{G}_x$  matrix, while small, is not necessarily zero given the analytical conditions. Bmad/Tao was used to optimize this to zero, so that a full first order spin match of the rotator was achieved; this result shows the benefits of using computational methods on top of an approximate analytical approach for minimal depolarization.

Figure 2 shows the polarization obtained from Monte Carlo tracking of the ESR, ESR with a vertical chicane, and ESR with a spin matched vertical chicane. Notably, there were some particles exceeding the longitudinal aperture and

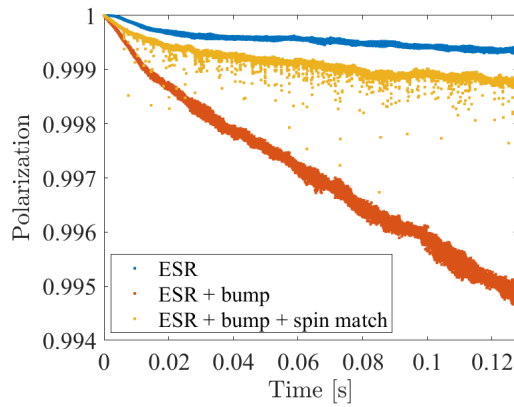


Figure 2: Polarization from Monte Carlo Bmad tracking for each lattice in the vertical chicane study.

Table 2: The polarization results for each lattice investigated in the vertical chicane study, with  $P_{bks}$  and  $\tau_{bks}$  calculated analytically in Bmad/Tao and  $\tau_{dep}$  calculated from Monte Carlo Bmad tracking.  $P_{dk}$  was then calculated with Eq. (5).

	ESR	ESR + bump	ESR + bump + spin match
$\tau_{bks}$	2226 s	1500 s	1500 s
$P_{bks}$	80.16%	53.92%	53.92%
$\tau_{dep}$	300.5 s	28.7 s	203.0 s
$P_{dk}$	9.53%	1.01%	7.53%

lost in the spin matched case. The depolarization rate  $\tau_{dep}^{-1}$  is obtainable from a linear fit of the polarization vs. time after the orbit has damped. Table 2 shows the resulting asymptotic polarization  $P_{dk}$  given the tracking data. The depolarization time and asymptotic polarization dropped significantly after introducing the vertical chicane. However, vertically spin matching the chicane restored the polarization significantly. This result suggests that the introduction of a vertical emittance creator into the ESR will require vertical spin matching to preserve polarization.

The equilibrium emittances obtained from analytical methods (radiation integrals with the vertical opening angle, PTC, and Bmad 6D calculation) were compared with those from the Monte Carlo tracking, as shown in Tables 3 and 4. Figure 3 shows the vertical emittances from tracking. A significant disagreement was observed in the horizontal emittance for the ESR + bump + spin matched lattice, and even greater disagreements observed in the vertical emittances for all lattices. The tracking emittances are believed to be the most physically accurate, however the great discrepancy between the analytical and tracking emittances is still being investigated.

## CONCLUSIONS

Bmad/Tao was used to achieve a full horizontal spin match of the rotator system in the ESR, showcasing the utility of

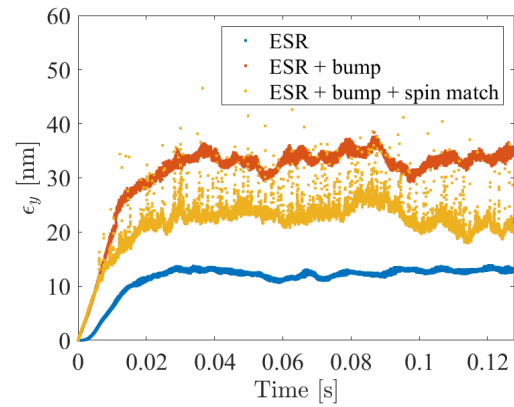


Figure 3: Vertical emittance from Monte Carlo Bmad tracking for each lattice in the vertical chicane study.

Table 3: Horizontal emittance  $\epsilon_x$  [nm] for each lattice in the vertical chicane study obtained through various methods.

	ESR	ESR + bump	ESR + bump + spin match
Rad. Integrals	27.762	25.026	37.216
PTC	28.372	25.561	43.406
Bmad 6D	27.694	24.951	42.863
Bmad Tracking	28.182	25.611	70.721

Table 4: Vertical emittance  $\epsilon_y$  [nm] for each lattice in the vertical chicane study obtained through various methods.

	ESR	ESR + bump	ESR + bump + spin match
Rad. Integrals	~0	7.550	7.690
PTC	~0	8.483	8.637
Bmad 6D	~0	7.571	7.700
Bmad Tracking	10.339	32.639	27.329

pairing computational methods with an approximate analytical approach to achieve maximum polarization. The insertion of a localized vertical dispersion bump in the ESR, necessary to increase vertical emittance and fix the electron beam size mismatch, was shown to have drastic effects on the polarization. However, spin matching the bump in Bmad/Tao proved to greatly remedy the losses introduced. Finally, a significant disagreement in the equilibrium emittances obtained from tracking vs. those from analytical methods was found. Future work involves resolving this emittance discrepancy and investigating different methods of vertical emittance creation (delocalized vertical dispersion creation, and both delocalized and localized coupling of the horizontal dispersion with the vertical) to determine which has a most easily resolvable effect on the polarization.

## REFERENCES

- [1] L. H. Thomas, "I. The kinematics of an electron with an axis," *Philos. Mag.*, vol. 3, no. 13, pp. 1–22, 1927, doi: 10.1080/14786440108564170
- [2] V. Bargmann, L. Michel, and V. L. Telegdi, "Precession of the polarization of particles moving in a homogeneous electromagnetic field," *Phys. Rev. Lett.*, vol. 2, pp. 435–436, 10 1959, doi: 10.1103/PhysRevLett.2.435
- [3] L. H. Thomas, "Recollections of the discovery of the Thomas precessional frequency," *AIP Conference Proceedings*, vol. 95, no. 1, pp. 4–12, 1983, doi: 10.1063/1.33853
- [4] G. H. Hoffstaetter, J. Ellison, and H. S. Dumas, "Adiabatic invariance of spin-orbit motion in accelerators," *Phys. Rev. Spec. Top. Accel Beams*, vol. 9, p. 014001, 2006, doi: 10.1103/PhysRevSTAB.9.014001
- [5] D. P. Barber, G. H. Hoffstatter, and M. Vogt, "The Amplitude Dependent Spin Tune and the Invariant Spin Field in High Energy Proton Accelerators," in *Proc. EPAC'98*, Stockholm, Sweden, Jun. 1998, <https://jacow.org/e98/papers/THP35G.pdf>
- [6] A. A. Sokolov and I. M. Ternov, "On Polarization and Spin Effects in the Theory of Synchrotron Radiation," *Sov. Phys. Doklady*, vol. 8, p. 1203, 1964.
- [7] B. W. Montague, "Polarized beams in high energy storage rings," *Phys. Rep.*, vol. 113, no. 1, pp. 1–96, 1984, doi: 10.1016/0370-1573(84)90031-0
- [8] V. N. Baier and V. M. Katkov, "Quantum effects in magnetic bremsstrahlung," *Phys. Lett. A*, vol. 25, no. 7, pp. 492–493, 1967, doi: 10.1016/0375-9601(67)90003-5
- [9] V. N. Baier, V. M. Katkov, and V. M. Strakhovenko, "Kinetics of radiative polarization," *Sov. Phys. JETP*, vol. 31, no. 5, p. 908, 1970.
- [10] Y. S. Derbenev and A. M. Kondratenko, "Polarization kinematics of particles in storage rings," *Sov. Phys. JETP*, vol. 37, pp. 968–973, 1973.
- [11] D. P. Barber and G. Ripken, "Computer Algorithms and Spin Matching," in *Handbook of Accelerator Physics and Engineering*. 2013, doi: 10.1142/8543
- [12] D. Sagan, *Bmad Manual*. 2022, <https://www.classe.cornell.edu/bmad/manual.html>
- [13] M. G. Signorelli and G. H. Hoffstaetter, *Different forms of first order spin-orbit motion and their utility in spin matching in electron storage rings*, 2021, doi: 10.48550/arXiv.2112.07607
- [14] V. I. Ptitsyn, *Spin Matching*, Spin Dynamics in Particle Accelerators, United States Particle Accelerator School, 2021.
- [15] V. I. Ptitsyn, *Spin matching derivation*, Brookhaven National Laboratory, 2021.
- [16] V. I. Ptitsyn and S. Tepikian, *Spin rotator design and spin matching*, EIC Workshop, Brookhaven National Laboratory, 2020.
- [17] A. W. Chao, "Evaluation of radiative spin polarization in an electron storage ring," *Nucl. Instrum. Methods*, vol. 180, no. 1, pp. 29–36, 1981, doi: 10.1016/0029-554X(81)90006-9